Supporting Information

CdTe Quantum Dots-Based Self-Supporting Films with Enhanced Stability for Flexible Light-Emitting Devices

Jin Wang, Li Wang*, XueQiong Su, DongWen Gao, HuiMin Yu.
College of Physics and Optoelectronics, Faculty of Science, Beijing University of Technology, Beijing 100124, China.
*Lwang.1@bjut.edu.cn

S1. Materials

Tellurium powder (Te, 99.9%), Selenium (Se, 99.9%), $Cd(NO_3)_2 \cdot 4H_2O$ (99%), Glutathione GSH (99%), Zinc chloride ($ZnCl_2$, 98%), Thiourea (AR,99%), Sodium borohydride $NaBH_4$ (99%), Sodium hydroxide NaOH (Ar, 95%), Hydrochloric acid Hcl (GR 36-38%), Polyvinyl alcohol (PVA, Mw~61000), Hydroxyethyl Cellulose (5000～6400 mpa), Tetraethyl orthosilicate (98%). All above chemicals were purchased from Macklin. ZnS target was purchased from ZhongNuo Advanced Material. All chemicals were used without further purification.

S2. Structural and optical characterization

Transmission electron microscope (TEM) image was recorded on a JEM-2100F electron microscope. The QDs solution was deposited on carbon-coated copper grids and air dried before imaging. **Powder X-ray diffraction (XRD)** measurements employed a Bruker D8 Advance with Cu Kα radiation (λ =1.5418 Å) in the 2θ range of 10–60°. To prepare a powder XRD sample, a higher concentrated nanocrystal solution (0.005 mmol/mL) was deposited on a monocrystalline silicon substrate and dried in air. **UV−vis absorption** spectra were obtained with a UV–Vis spectrophotometer (G1103A, Agilent Technologies). **Fluorescence calibration spectra** were obtained with F-4600, HITACHI, Japan. The concentration of CQDs is 0.001mol/L, and the intensity represents the PL intensity of CQDs. **Fluorescence stability test spectra** were collected with a spectrophotometer (USB 4000, Ocean Optics) equipped with a 450 nm continuous wave laser. All PL intensity measurements were repeated 5 times and averaged. **Scanning electron microscopic (SEM)** images were acquired by the JEOL JSM-6700F at a voltage of 15 kV and an electron current of 92 μA.

S3. Synthesis of CdTe CQDs

Firstly, 1 mmol Te powder and 4 mmol $NaBH_4$ were dissolved in 2 ml degassed deionized water and stirred for several hours to prepare NaHTe solution. Then, GSH (0.625 mmol) and $Cd(NO_3)_2 \cdot 4H_2O$ (0.25 mmol) were dissolved in 25 mL deionized water to prepare Cd^{2+} precursor solution. The mixture was adjusted to pH 8.5 with NaOH (1 mol/L). The NaHTe solution (125 μL) was injected into N_2 saturated Cd^{2+} solution, the mixed solution was refluxed at 100 ℃ for 10, 20, 30, 40 and 60 min. They were labeled CdTe 1, CdTe 2, CdTe 3, CdTe 4, CdTe 5, respectively. CdTe 5 with 595 nm emission wavelength was selected for stability test.

S4 Structural characterization

TEM images of a representative CdTe CQDs are shown in figure S1a and S1b. Figure S1a shows that CdTe CQDs are circular or elliptical with the size of 6.05 nm and have good dispersion. Figure S1b clearly shows the lattice stripes of CdTe with a lattice spacing of 0.37 nm, corresponding to the (111) crystal plane of CdTe (CdTe #75-2086). The structure of CdTe is further shown by XRD in figure S1c. The 26° corresponds to the (111) crystal planes and the 44° corresponds to the overlap of crystal planes (220) and (311). The CQDs are consistent with the cubic phase sphalerite structure.

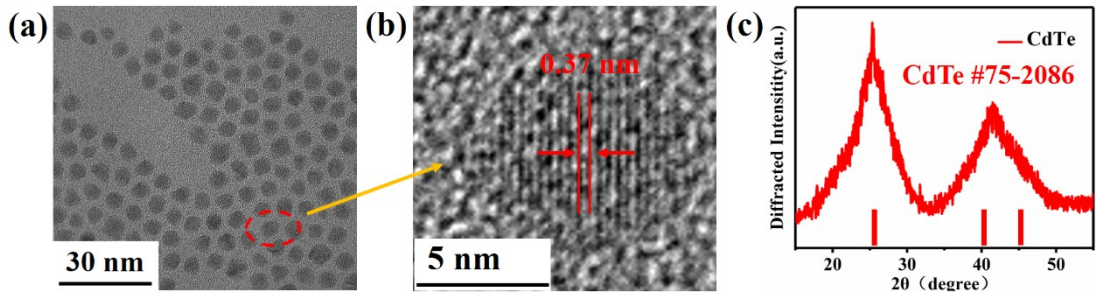

Figure S1. (a) TEM images of CdTe. (b) HRTEM images of CdTe (c) XRD of the CdTe.

S5 Size distribution comparison of CdTe just prepared and placed for six months

As can be seen in figure S2a and S2b, the dispersion and lattice clarity of the CdTe just prepared are better than that of the CdTe placed for six months, which fully illustrates the characteristics of aged CdTe CQDs. The shedding of ligands leads to the cluster phenomenon of CQDs. Figure S2c and S2d clearly show that the aged CdTe size distribution is relatively dispersed, but the average size does not change significantly, which is the reason why the PL emission maximum of the aged CdTe spectrum is unchanged but the spectral is widened.

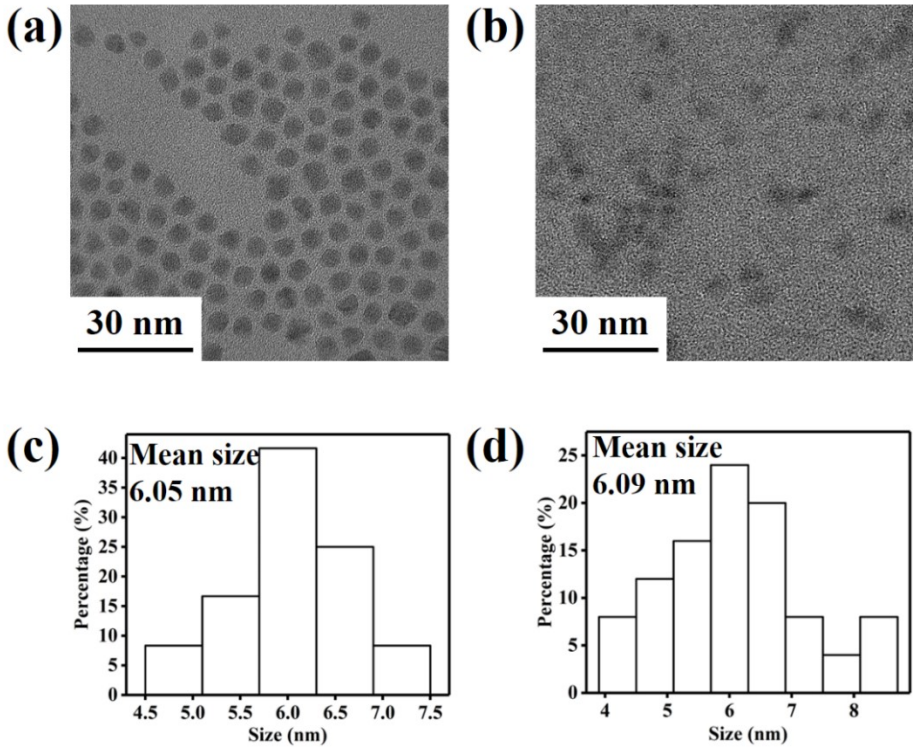

Figure S2. (a) TEM images of CdTe just prepared. (b) TEM images of CdTe placed for six months. (c) Size distribution of CdTe just prepared. (d) Size distribution of CdTe placed for six months.

S6. CdTe solution in acid

The changes of PL intensity and EM were continuously observed by the spectrometer in situ. When the pH value of the CQDs solution is adjusted, the light source is covered. After the pH value is adjusted, the light source irradiates the CQDs solution for 1 min, and then the PL intensity is recorded. It can be ensured that the PL intensity measured at each pH value is not affected by the irradiation and erosion time. Figure S3 shows the CdTe solution in acid and alkaline environment.

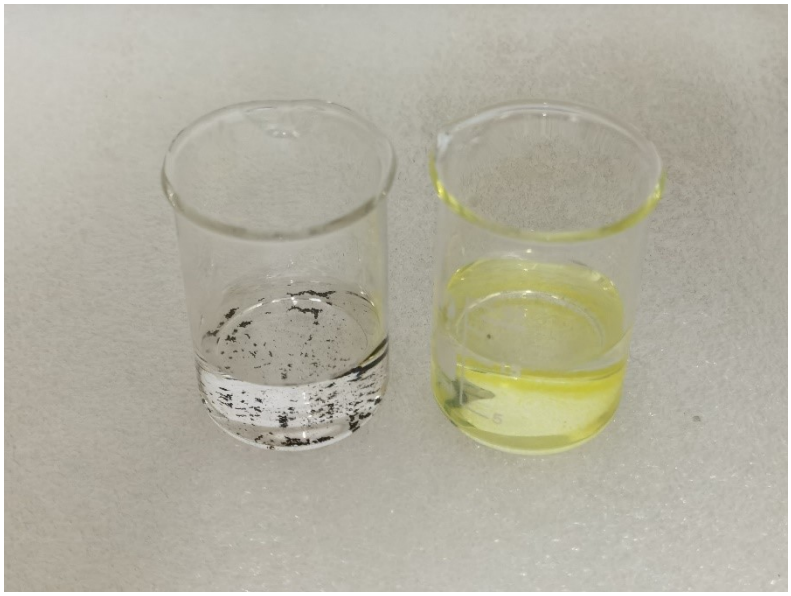

Figure S3. CdTe in acid (left) and alkaline environment (right).

S7. PL emission spectra variation of CdTe before and after freezing

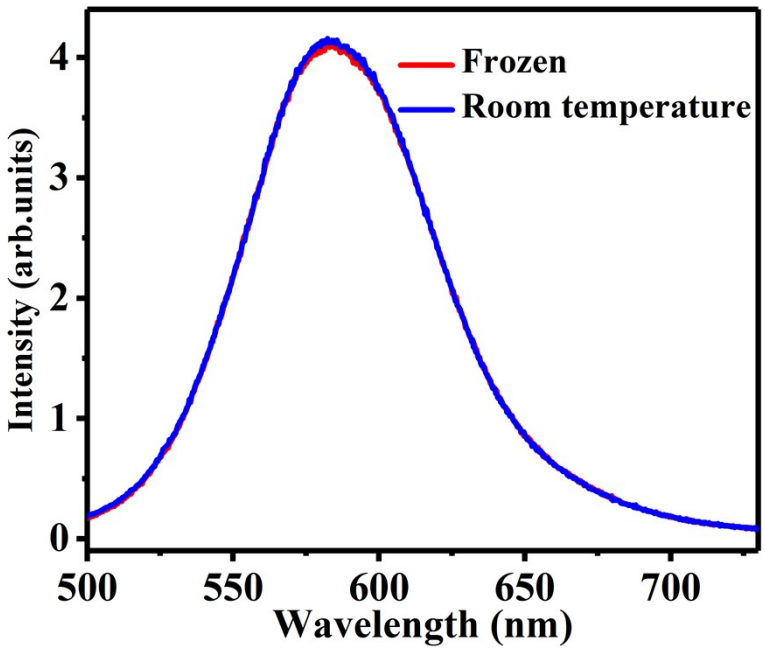

Figure S4. (a) PL emission spectra variation of CdTe before and after freezing.

S8. CdTe before freezing and after freezing

Figure S5. CdTe before freezing (left) and after freezing (right).

S9. The fluorescence color of the CdTe, CdTe/CdSe, CdTe/CdSe/ZnS

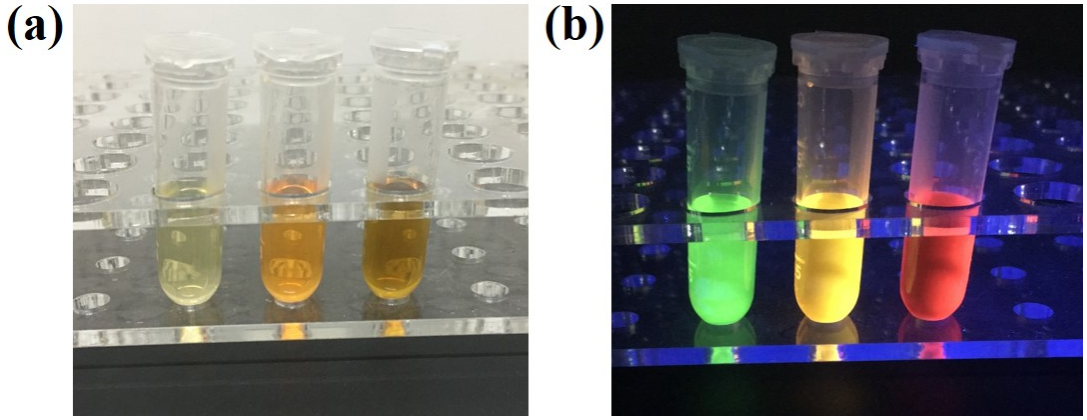

Figure S6. The fluorescence color of the CdTe, CdTe/CdSe, CdTe/CdSe/ZnS under (a) natural light and (b) ultraviolet light.

S10. The band gap width of the CdTe, CdTe/CdSe, CdTe/CdSe/ZnS

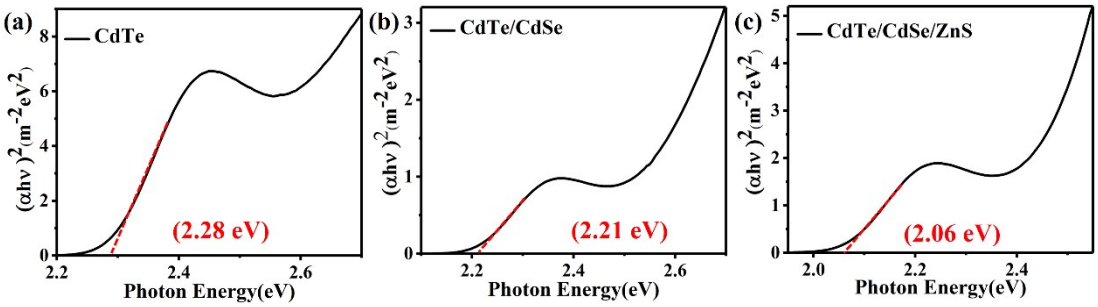

Figure S7. The band gap width of the (a) CdTe, (b) CdTe/CdSe and (c) CdTe/CdSe/ZnS.

S11. TEM image and the diameter counting of CdTe, CdTe/CdSe, CdTe/CdSe/ZnS.

We randomly selected 40 of the three kinds of CQDs in the TEM images for size distribution

statistics, and obtained the average size of the three kinds of CQDs.

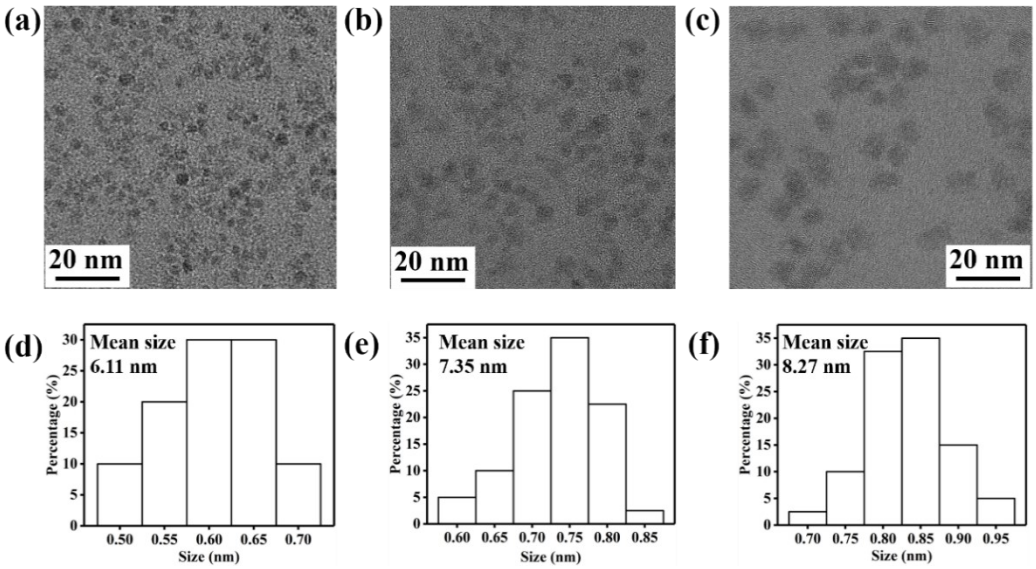

Figure S8. (a), (b), (c) TEM image of CdTe, CdTe/CdSe, CdTe/CdSe/ZnS. (d), (e), (f) Diameter counting of CdTe, CdTe/CdSe, CdTe/CdSe/ZnS.

S12. The change of the PL emission spectra of the CdTe/CdSe/ZnS and CdTe/SiO_2

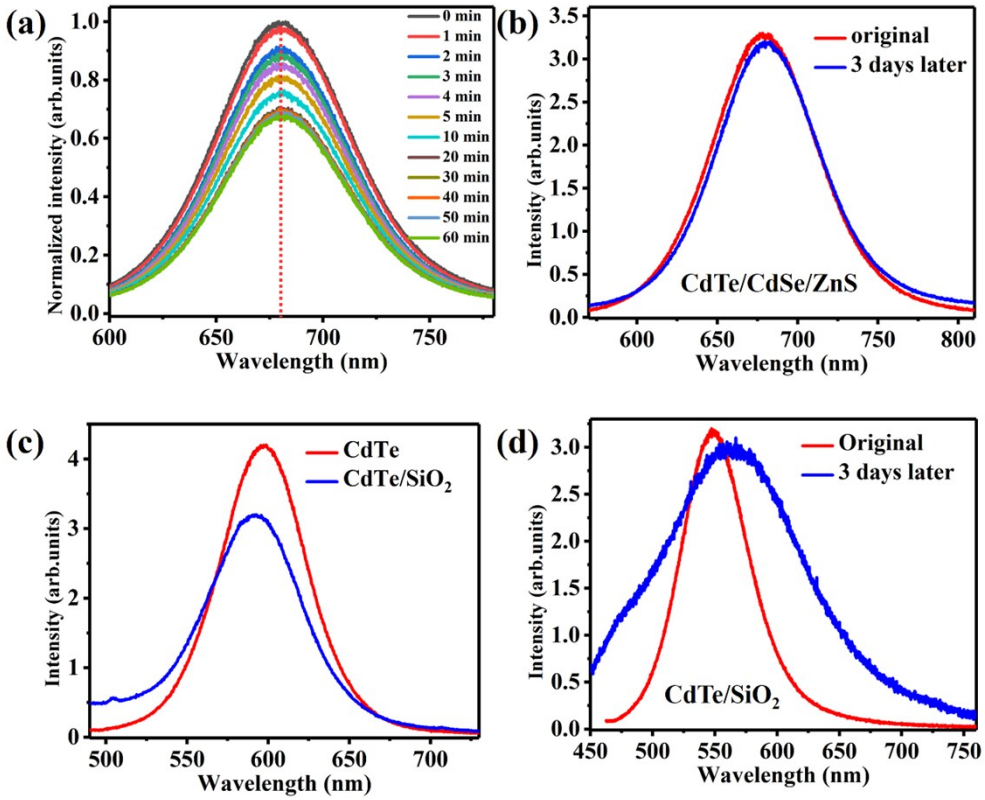

Figure S9. (a) Variation of of the CdTe PL emission intensity with 450 nm continuous wave laser illumination time. (b) The change of the PL emission spectra of the CdTe/CdSe/ZnS 3 days later. (c) PL emission spectra of the CdTe/SiO_2. (d) The change of the PL emission spectra of the CdTe/SiO_2 3 days later.

S13. The comparison of PL intensity among CdTe/CdSe/ZnS, CdTe/CdSe, CdTe and CdTe/SiO_2

The PL intensity of CdTe/CdSe is weaker than that of CdTe because of the indirect band gap of type II CQDs. After the ZnS shell with wide band gap is covered, the CdTe/CdSe/ZnS CQDs becomes a direct band gap as a whole. The double-layer core-shell passivation structure makes its PL intensity significantly higher than that of the initial CdTe. Although SiO_2 shell can fully play the role of surface activation, and the surface ligands are better isolated from air, the thickness of about 1 μm greatly increases the loss of fluorescence, and the PL intensity decreases compared with the initial CdTe.

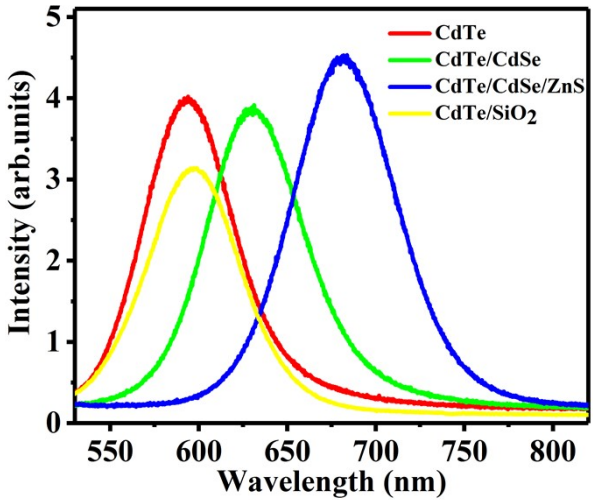

Figure S10. The comparison of PL intensity among CdTe/CdSe/ZnS, CdTe/CdSe, CdTe and CdTe/SiO_2.

S14. CdTe CQDs film under optical microscope

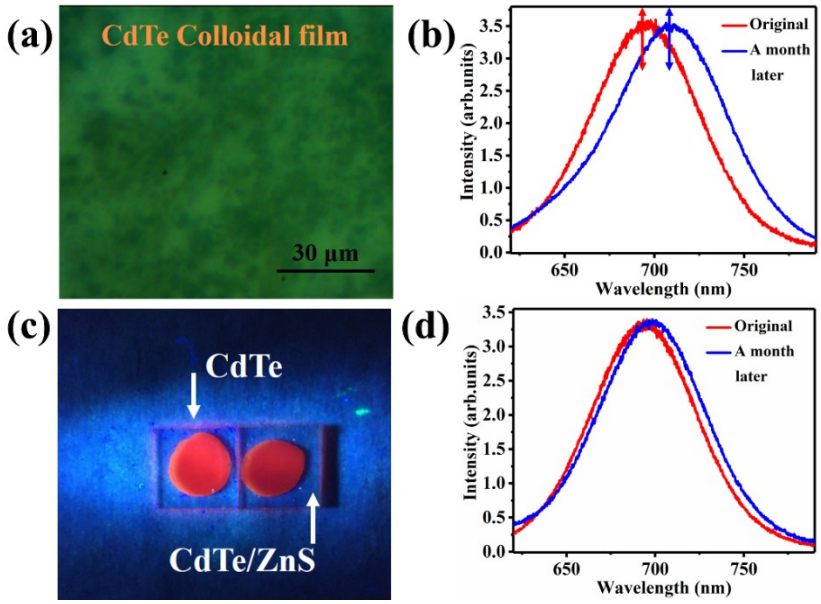

Figure S11. (a) CdTe CQDs film under optical microscope. (b) The change of the PL emission spectra of the CdTe film a month later. (c) The fluorescence color of CdTe film and CdTe/ZnS film under ultraviolet light. (d) The change of the PL emission spectra of the CdTe/ZnS film a month later.

S15. The fluorescence color of the CdTe/PVA film and CdTe/hydroxyethyl cellulose

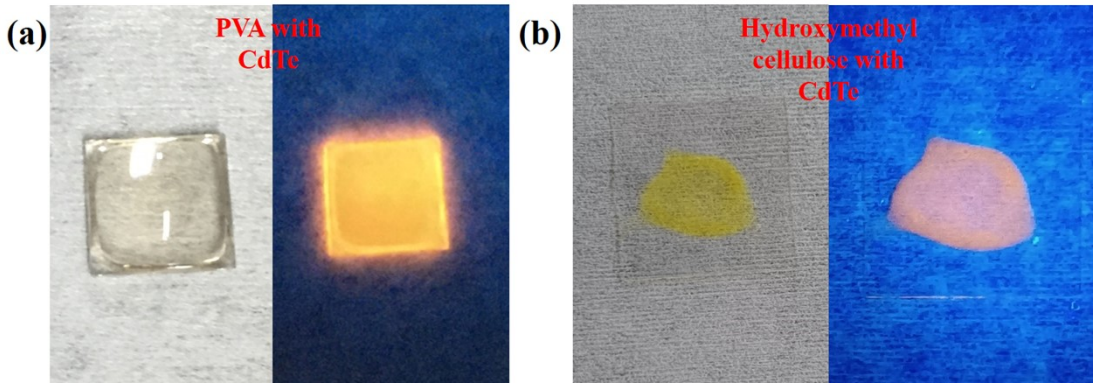

Figure S12. (a) The fluorescence color of the CdTe/PVA film under natural light and ultraviolet light. (b) The fluorescence color of the CdTe/hydroxyethyl cellulose film under natural light and ultraviolet light

S16. Changes of CdTe/PVA film and CdTe/hydroxyethyl cellulose spectra with time

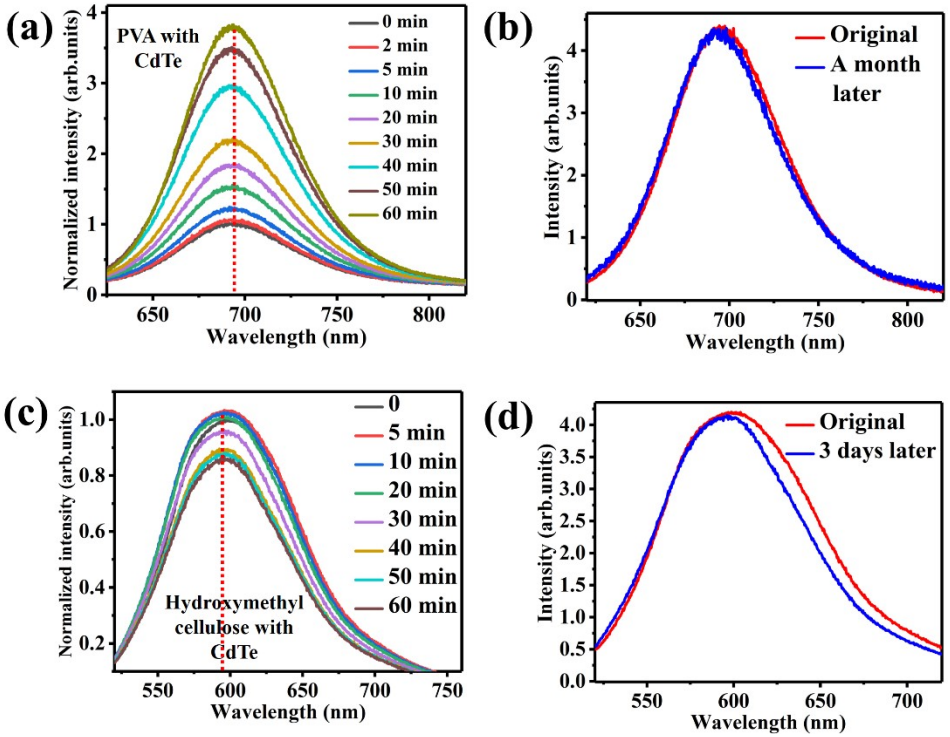

Figure S13. (a) Variation of of the CdTe/PVA film PL emission intensity with illumination time. (b) The change of the PL emission spectra of the CdTe/PVA film a month later. (c) Variation of of the CdTe/hydroxyethyl cellulose film PL emission intensity with illumination time. (d) The change of the PL emission spectra of the CdTe/PVA film a month later.

S17. Variation of of the CdTe film, CdTe/PVA film, CdTe/hydroxyethyl cellulose film PL emission intensity with injection times of HCl.

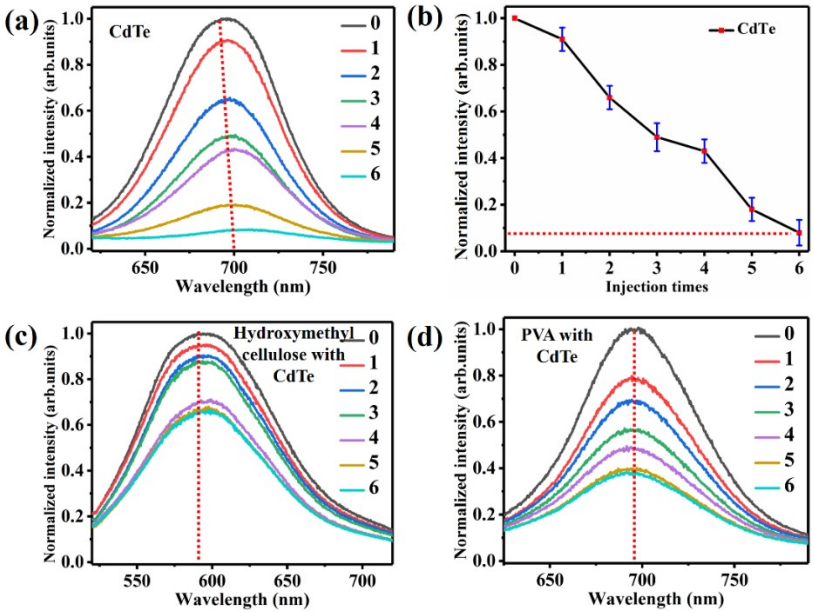

Figure S14. (a) Variation of of the CdTe film PL emission intensity with injection times of HCl. (b) Linear relationship between PL emission intensity of the CdTe film and injection times of HCl. (c) and (d) Variation of of the CdTe/PVA film and CdTe/hydroxyethyl cellulose film PL emission intensity with injection times of HCl.

S18. Wavelength adjustment and modulation

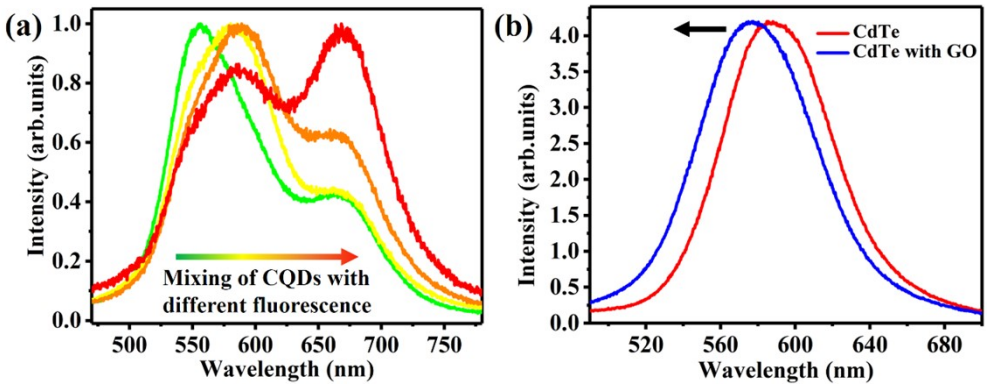

Figure S15. (a) Wavelength adjustment by mixing different fluorescent CdTe solutions. (b) The wavelength of CdTe is modulated by graphene oxide QDs.

S19. Different fluorescent films superimposed to adjust chromaticity and wavelength

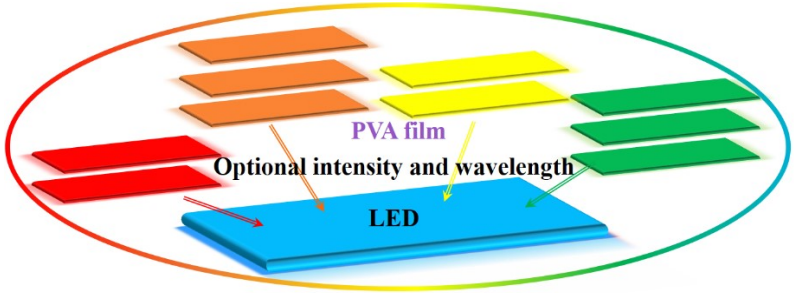

Figure S16. Different fluorescent films superimposed to adjust chromaticity and wavelength

S20. CSPZ flexible film characteristics

Figure S17a and S17b show that the curved CSPZ flexible film under natural light and ultraviolet light. As shown in figure S17c. the PL intensity of the area covered by ZnS film is lower than that without ZnS film. This is because ZnS has slight absorption in the visible fluorescence band, but will not change the original chromaticity of CQDs fluorescence. It plays a good role in passivating the CQDs on the surface layer of PVA polymer to avoid lattice defects caused by photo-oxidation. The SiO_2 microspheres in figure S15d have obvious monodispersity in the film. The light energy distribution of the cross section of SiO_2 microsphere is observed by simulation as shown in the inset of figure S17d. The WGM oscillation in the spherical micro cavity would result in the optical field being confined along the SiO_2 microsphere interface. As shown in figure S17e, two peaks are selected for calculation. The peak is fitted by Gauss to obtain the FWHM and the average FWHM is 1.4 nm. The same excitation light source (343 nm, 1 ns, 100 Hz) was used to irradiate the PVA/CdTe film without SiO_2. With the increase of pump intensity, the PL intensity increased but no narrow band appeared as shown in the figure S15f

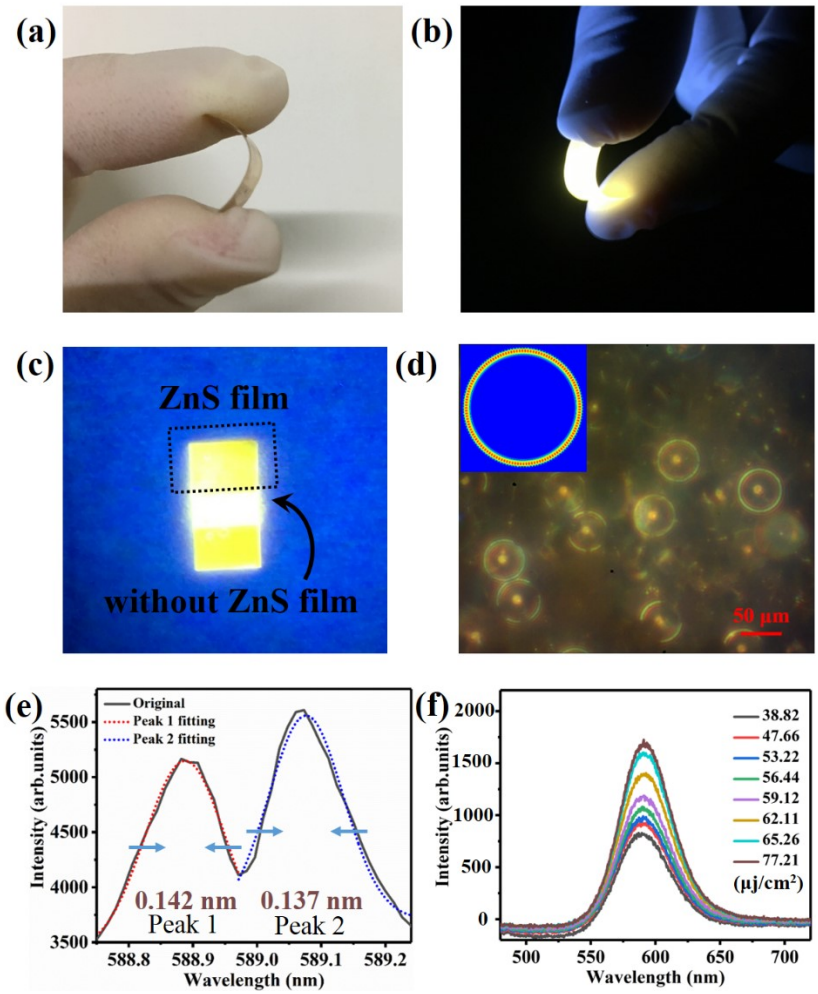

Figure S17. (a) and (b) The fluorescence color of the CSPZ flexible film under natural light and ultraviolet light. (c) ZnS film coated on PVA film. (d) SiO_2 microspheres in CSPZ film under optical microscope and the effect of local field enhancement of SiO_2. (e) The numerical fitting of full width at half maximum (FWHM). (f) Emission spectra of PVA/CdTe film without SiO_2 under different pump power.